Supporting Information

Frequency Domain Detection of Biomolecules using Silicon Nanowire Biosensors

Gengfeng Zheng,[*,†] *Xuan P.A. Gao,*[*,‡] *and Charles M. Lieber*[§,‖]

[†]Laboratory of Advanced Materials and Department of Chemistry, Fudan University, Shanghai, 200433, People's Republic of China, [‡]Department of Physics, Case Western Reserve University, Cleveland, Ohio 44106, [§]Department of Chemistry and Chemical Biology, and [‖]Division of Engineering and Applied Science, Harvard University, Cambridge, Massachusetts 02138.

* Corresponding authors: gfzheng@fudan.edu.cn and xuan.gao@case.edu

This file contains:

Methods

Methods

Nanowire synthesis, device fabrication, and functionalization. The silicon nanowire (SiNW) synthesis, field-effect transistor (FET) device fabrication, modification of device surfaces with receptors have been described previously.[1] In brief, SiNWs were synthesized by nanocluster-catalyzed chemical vapor deposition, with 20-nm-diameter gold nanoparticles used as catalysts. Silane (SiH_4) and diborane (B_2H_6) were used as gas reactants, with a B:Si atomic ratio of 1:4000 in gas phase to yield p-type materials. SiNW FET devices were fabricated on a single silicon <100> substrate with 600 nm thick SiO_2 layer. Metal electrode contacts were defined by photolithography, followed by 60 nm Ni metal deposition and subsequent passivation of the Ni contacts with ca. 50 nm thick Si_3N_4 layer. The SiNW surfaces were modified with monoclonal antibodies via aldehyde silane conjugation followed by ethanolamine passivation.[1] The prostate specific antigen (PSA) samples were diluted in the assay buffer (100 μM phosphate buffer solution containing 100 μM KCl, pH = 7.4) prior to sensing measurements, and were delivered to the SiNW FET sensor arrays using a flexible PDMS polymer microfluidic channel sealed to the device chip. A typical solution flow rate is 0.4 – 0.5 ml/hour.

Nanowire sensor measurements. Conventional time domain conductance measurements were carried out in the voltage-biased mode,[2] in which a constant source-drain voltage (50 mV, either AC or DC) was applied, and the current flowing through the SiNW FET devices was measured by a current pre-amplifier (Model 1211, DL Instruments LLC.). Frequency domain experiments were carried out in the current-biased mode[2] due to larger bandwidth of the voltage

pre-amplifier at the requisite signal gain. A stable current was provided by an Agilent DC voltage supply (full output voltage: 0 – 120 V, typically we used 30 – 60 V) and 500 MΩ resistor in series with the NW, where the voltage drop across the device was amplified by a voltage amplifier (Model SR560, Stanford Research Systems Inc.) with bandwidth of 1 MHz. The power spectrum of the amplified voltage across NW was then collected by a FFT spectrum analyzer (Model SR760, Stanford Research Systems Inc.).

Models of frequency domain studies. Two noise sources were considered for the analysis of noise mechanisms in SiNW FET biosensors: (1) equivalent gate voltage noise from both the biomolecule-receptor binding/unbinding, and (2) thermal fluctuations. First, we analyzed the gate voltage noise induced by biomolecules binding/unbinding on SiNW surface using a two-level model. Second, we considered the gate voltage noise induced by thermal fluctuations when the NW surface has bound biomolecule layers.

(1) Noise associated with molecule binding/unbinding. The basic assumptions for this model are (i) a total of N binding sites (antibody receptors on a given NW device), where (ii) N_0 are conjugated with target antigen molecules, and the effective gate voltage induced by the binding of N_0 antigens is V_p, and (iii) antigen molecules are independent, and each bound antigen yields an effective gate voltage of V_m.[3] Modeling the on/off state switching of the single molecule binding/unbinding is similar to the random telegraph signal in a MOSFET.[4] In this context, binding/unbinding of a single antigen molecule yields a Lorentzian power spectral density in gate voltage:

$$\delta V_p^2(f) = \frac{4V_m^{\ 2}}{(\tau_0 + \tau_1) f_c^2 [1 + (2\pi f / f_c)^2]} \qquad (1)$$

where $f_c = 1/\tau_0 + 1/\tau_1$, and τ_0 , τ_1 stand for the average binding and unbinding times, respectively. The transition probability (per unit time) from "on" to "off" state is $1/\tau_1$ and from "off" to "on" state is $1/\tau_0$, as shown in Figure S1.

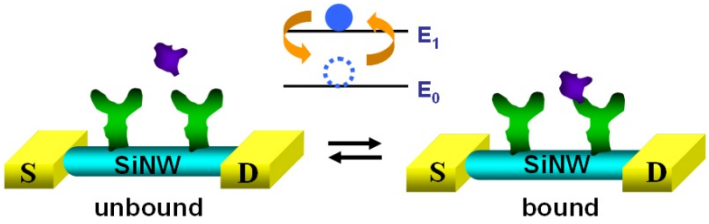

Figure S1. Schematic of antigen (purple color) binding and unbinding on a SiNW FET sensor surface functionalized with antibodies (green color), which resembles as a two-level-state system.

The rate equation for N sites is:

$$\frac{dN_0}{dt} = \frac{1}{\tau_0} \times (N - N_0) - \frac{1}{\tau_1} \times N_0,$$

and yields

$$N_0 = \frac{N/\tau_0}{1/\tau_0 + 1/\tau_1}$$

at equilibrium. Comparing to the conventional rate equation:

$$\frac{dN_0}{dt} = k_a c \times (N - N_0) - k_d \times N_0$$

we can associate $1/\tau_0 = k_a \times c$ and $1/\tau_1 = k_d$, with c as the antigen (PSA) concentration. Thus f_c in Eq. (1) should be equivalent to $(k_a \times c + k_d)$. This is consistent with the idea of using frequency

spectrum of fluctuations to study chemical reaction rates, proposed more than 30 years ago.[5] Since $k_a \sim 10^6$ $M^{-1}s^{-1}$ and $k_d \sim 10^{-2}$ s^{-1} for PSA/antibody conjugation, in the concentration range $c \leq$ nM, the calculated f_c is about 10^{-2} Hz. This value is outside the typical frequency range of our measurements (1 Hz – 100 kHz), and is significantly different from our measured characteristic Γ (a few kHz). In addition, due to the existence of $1/f$ noise background, a 10^{-2} Hz plateau would most likely be dominated by the $1/f$ curve. Under a different molecule recognition system that has a larger k_a and a higher concentration, it might be possible to achieve a larger f_c, thus being able to test the applicability of this model.

(2) Thermal fluctuation driven noise. By treating the NW-receptor-target layer as a macroscopic system in thermal equilibrium with the environment, we can estimate the gate voltage noise due to the thermal fluctuations.[6,7] The equivalent circuit for the NW FET biosensor is shown in Figure S2. Here we discuss the effect of antigen binding on the gate voltage noise power spectral density using a circuit diagram shown in Figure S2, where C_{ox}, C_{ab} and C_{dl} are the capacitances of the silicon dioxide, the antibody layer, and the electrical double layer at the NW biosensor-water interface, and R_b is the resistance of bulk solution between NW and the solution gate. Binding of antigens adds an extra layer of capacitance and resistance between the electrolyte double layer and the antibody-oxide dielectric layer to the NW surface, where C_{PSA}, R_{PSA} represent the capacitance and resistance of the PSA layer, respectively.

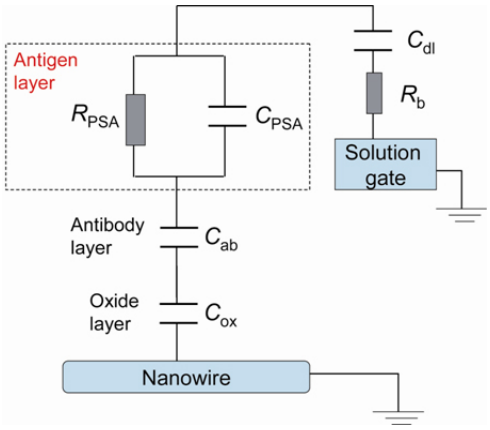

Figure S2. Schematic of the equivalent circuit for NW FET biosensor after the binding of antigens (PSAs) on antibodies.

The voltage (Johnson) noise of R_{PSA} in Figure S2 creates a gate voltage noise δV_g. Because δV_g is coupled to the NW transport through various resistors and capacitances, the RC time constant $\tau = RC$ will set a high frequency cutoff in $S_{Vg}(f)$, where the power spectral density of δV_g in the frequency domain $S_{Vg}(f)$ will exhibit a Lorentzian shape with corner frequency $f_c = 1/2\pi\tau$, as follows:[6-8]

$$\delta V_g^2(f) = \frac{4k_B TR}{1+(2\pi f\tau)^2} \qquad (2)$$

with τ being the overall RC time constant of Figure S2 determined by the Johnson noise source and the combined capacitance. As the conductivity of an electrolyte solution is much higher than that of protein layers,[9] we assume $R_b << R_{PSA}$, and get:

$$\tau \approx R_{PSA}[C_{PSA} + 1/(C_{dl}^{-1} + C_{ab}^{-1} + C_{ox}^{-1})] \qquad (3)$$

Since all the capacitances in Eq. (3) are on order of fFs for the geometry of NW devices,[10] to obtain $\tau \sim 0.3$ ms measured in our experiment, the resistance of the antigen layer (R_{PSA}) needs to

be on the order of tens of GΩs, which is possible in molecule layers,[11] and consistent with our assumption that $R_b << R_{PSA}$.

From this analysis, we can see that both the antibody concentration (which determines C_{ab}) and the antigen concentration can affect f_c. However, for antigen concentration > 0.15 pM, the spacing between two neighboring antigen molecules on the NW is smaller than the Debye length of the buffer used (~ 50 nm). As a result, the capacitance of the antigen layer will saturate for antigen concentrations > 0.15 pM. This explains our observation that the corner frequency of the Lorentzian noise of NW sensor with conjugated PSA-PSA antibody on surface only depends on the coverage density of PSA antibodies, but not PSA in the concentration range tested here.

This model of Lorentzian noise induced by antigen-antibody binding is further supported by the noise spectrum measurements for a different type of antibody-antigen system. Figure S3 shows noise measurement of a SiNW FET sensor in the presence of 0.15, 5 and 150 pM cholera toxin sub-unit B (CTB). Here the SiNW sensor surface was modified with CTB-antibodies under conditions similar to Figure 2 of the main manuscript (the "medium antibody coverage" case). This CTB functionalized sensor exhibits a corner frequency $\Gamma \sim 2500$ Hz in the presence of CTB, quite different from the corner frequency for the PSA sensors ($\Gamma \sim 3800$ Hz). In addition, similar to the PSA sensing experiment, changing the CTB concentration by three orders of magnitude did not lead to a measurable change of the corner frequency Γ for CTB concentrations > 0.15 pM. These results further point to the importance of the properties of the biomolecules on the noise spectrum of a NW FET biosensor. In summary, the Lorentzian noise of NW FET biosensors is consistent with the thermal noise of antigen layer bound to the surface of nanowire.

Resistance of GΩs is required for the antigen layer to obtain characteristic corner frequency of kHz for the Lorentzian noise. In the future, a more quantitative understanding of the noise spectra require further detailed understanding of C_{ab}, C_{PSA}, and R_{PSA}.

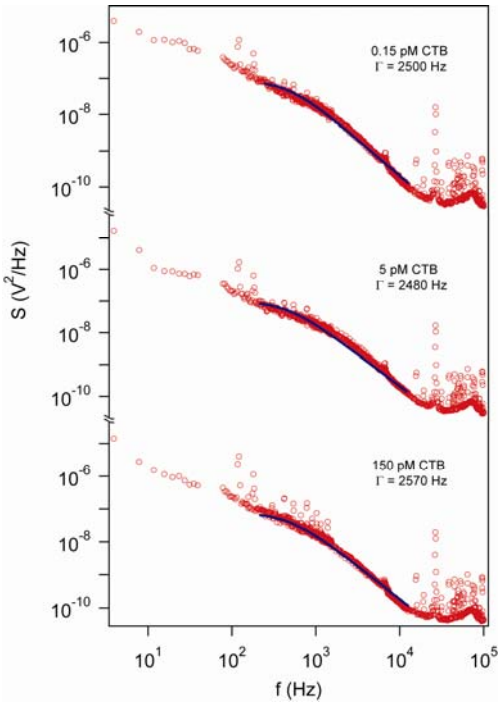

Figure S3. The power spectra of the SiNW FET sensor with CTB-antibody modification, in buffer solutions with different CTB concentrations, 0.15 pM, 5 pM, 150 pM. All the spectra show Lorentzian noise with characteristic corner frequency (Γ) ca. 2500 Hz for all the different CTB concentrations.

References:

(1) Patolsky, F.; Zheng, G.; Lieber, C. M. *Nat. Protocols* **2006**, *1*, 1711-1724.

(2) Collins, P. G.; Fuhrer, M. S.; Zettl, A. *Appl. Phys. Lett*. **2000**, *76*, 894-896.

(3) It is proper to view the charged molecules on a NW as charges along a line. The gating effects from individual molecules should add in series instead of parallel. So the effective gate voltage from each antigen molecule is not simply V_p/N_0. Instead, we define this effective gate voltage as V_m.

(4) Kirton, M. J.; Uren, M. J. *Adv. Phys.* **1989**, *38*, 367-468.

(5) Feher, G.; Weissman, M. *Proc. Natl. Acad. Sci. USA* **1973**, *70*, 870-875.

(6) Hassibi, A.; Navid, R.; Dutton, R. W.; Lee, T. H. *J. Appl. Phys.* **2004**, *96*, 1074-1082; **2005**, *98*, 069903.

(7) In a related system where neuron cells adhered on top of planar silicon transistor, thermal fluctuations were used to explain the extra Lorentzian noise induced by neuron adhesion. Voelker, M.; Fromherz, P. *Phys. Rev. Lett.* **2006**, *96*, 228102.

(8) Note that although $1/f^2$ type dependence in $S_{Vg}(f)$ can also be due to charge transfer process at a faradic electrode surface as described in ref. 6, we follow the conventional approach of modeling NW as a non-faradic electrode in which all the noises source originate from the thermal noise of the dissipative (resistive) components in the circuit.

(9) Resistivity of a few nm thick molecular layers is very high (>10^{12} Ω/nm^2, see ref.11). Therefore, it is reasonable to assume $R_b << R_{PSA}$, for the 100 μM buffer solution used.

(10) Garnett, E. C.; Tseng, Y. C.; Khanal D. R.; Wu, J. Q.; Bokor, J.; Yang, P. D. *Nat. Nanotechnol.* **2009**, *5*, 311-314.

(11) Bang, G. S.; Chang, H.; Koo, J. -R.; Lee, T.; Advincula, R. C.; Lee, H. *Small* **2008**, *4*, 1399-1405.